

WAVEGUIDE DISCONTINUITIES

Any deviation from uniformity along the longitudinal axis of a waveguide constitutes a discontinuity. Discontinuities are unavoidably present in any microwave circuit, either unintentionally or for the purpose of performing a prescribed function. In the former case one usually tries to minimize the unwanted mismatching due to the discontinuity, while in the latter case the discontinuity is instrumental in the design of a specific component. A typical example of the former category is a waveguide bend, while a metal diaphragm is representative of the latter.

The electromagnetic (*EM*) field incident on a discontinuity is partly reflected and partly transmitted, while reactive energy is stored in the proximity of the discontinuity. If lossy materials are present, some power may be lost, and in case of open structures, some power may be radiated.

The electromagnetic analysis of a discontinuity involves the solution of Maxwell's equations with appropriate boundary conditions. Analytical techniques for the solution of boundary-value problems in electromagnetics are presented and discussed in a number of classical textbooks, such as Refs. 1,2,3,4. Extensive discussion on waveguide discontinuities and their general properties can be found in Refs. 5 and 6. With the exception of a few simple cases, for which an analytical solution can be found, some sort of approximation, either analytical or numerical, is necessary to express the solution of the electromagnetic problem.

The problem can be attacked using either rigorous or approximate approaches. Rigorous approaches differ from approximate ones in that the exact solution can, in principle, be obtained with any degree of accuracy. In contrast, the accuracy obtainable with approximate approaches cannot be pushed beyond intrinsic limits.

Although a number of rigorous methods have been developed for the solution of electromagnetic structures and available computational resources are extremely powerful, rigorous solutions are often too cumbersome for many practical purposes. Approximate solutions, though less accurate, may be more advantageous as they are much simpler to achieve.

A large number of numerical methods for the analysis of waveguide discontinuities and, more generally, for the solution of microwave boundary-value problems have been published. See, for instance, Refs. 7,8,9,10.

One of the most powerful and popular methods for solving waveguide discontinuities is the modal analysis or mode-matching technique (11,12,13). Besides being a rigorous approach, it lends itself to a physical interpretation of the electromagnetic field behavior due to the presence of the discontinuity and leads to the so-called microwave network formalism. By virtue of the equivalence between waveguide modes and transmission lines, the electromagnetic description of the discontinuity can be translated in terms of an equivalent network. The full computation of the electromagnetic field in the structure is more than is usually required. A terminal description of the discontinuity as seen from the waveguides connected to it is all that is necessary. This makes it possible to express a complicated electromagnetic problem in terms of a more familiar circuit theory model.

The description of waveguide discontinuities is introduced on the basis of the modal analysis approach. This leads to the generalized description of the discontinuity as a multiport network using impedance, admittance, or the scattering matrix (or other matrix descriptions). General properties of waveguide discontinuities are then presented, as is a categorization of various classes of waveguide discontinuities. The concept of

2 WAVEGUIDE DISCONTINUITIES

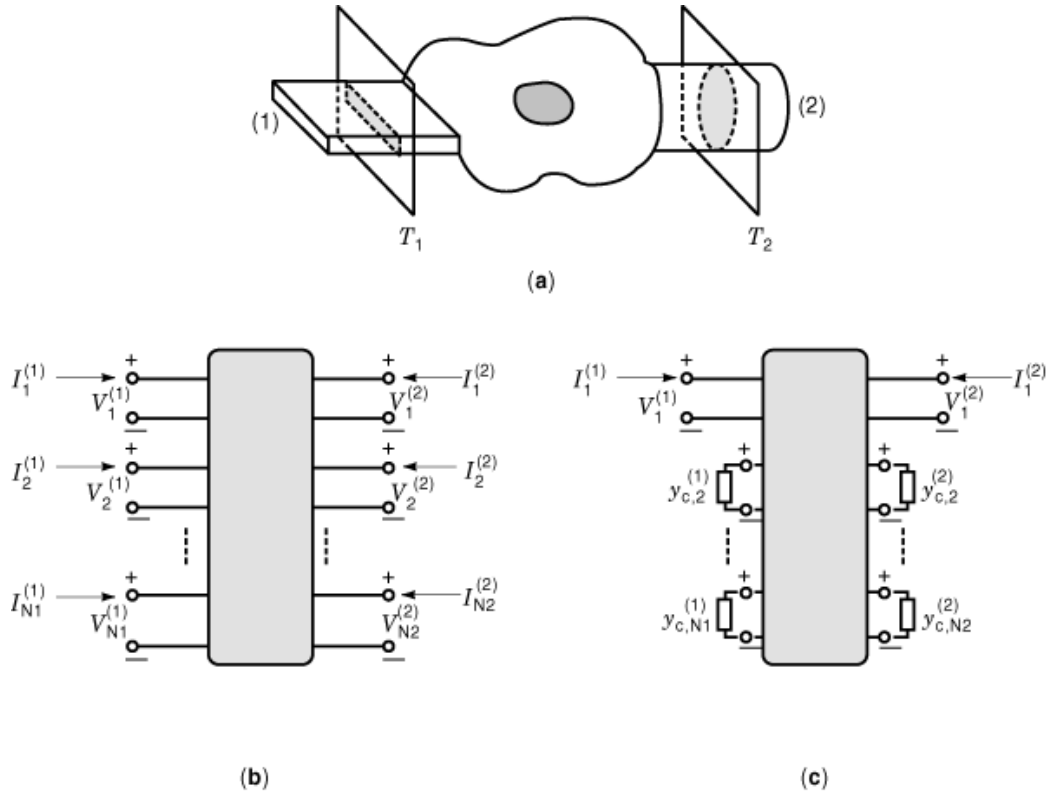


Fig. 1. Generic, two-port waveguide discontinuity and its network representations. (a) waveguide discontinuity; (b) multiport description; (c) reduced two-port description.

interacting and isolated discontinuities, which is familiar to the microwave engineer but has no counterpart in conventional circuit theory, is also illustrated by a specific example.

Description of Waveguide Discontinuities

Figure 1(a) depicts a generic discontinuity with two outputs. The structure consists of a central region bounded by metallic walls, connected to two uniform waveguides. In the present discussion, the structure of Fig. 1(a) is taken as an example, with the extension to more general cases, for example, multiple outputs and magnetic walls, being straightforward. Two reference planes T_1 and T_2 define the boundary between the discontinuity region and the input and output waveguides. Various types of obstacles, either lossless (perfectly conducting or perfect dielectric materials) or lossy, isotropic or anisotropic, may be present in the discontinuity region.

When an electromagnetic field impinges on the discontinuity from one or both waveguides, part of the associated energy is reflected, part is dissipated within the discontinuity, and part is transmitted to the other waveguide. Reactive energy is stored in the discontinuity region and in the nearby waveguide region.

In most practical cases, what is required is just a terminal description of the discontinuity rather than the detailed knowledge of the electromagnetic field distribution within the discontinuity. It is worth recalling that the field distribution in a waveguide results from the superposition of its normal modes. In normal

operating conditions, the dominant mode is the only propagating mode, while all higher-order modes, excited at the discontinuity, are exponentially decaying. Usually, the terminal planes are placed far enough from the discontinuity in such a way that only the dominant modes have nonnegligible amplitudes. In such conditions, a terminal description of the discontinuity can be obtained by writing the equations relating the field quantities at the two terminal planes. Such relations may take the form of a 2×2 impedance matrix if the electric fields are expressed in terms of the magnetic fields, or the form of an admittance matrix if the magnetic fields are expressed in terms of the electric fields. As is specified later, in fact, electric and magnetic fields can be replaced by equivalent voltage and current amplitudes. In a number of important cases, however, the terminal planes must be placed near the discontinuity region, so that the field distribution cannot be reduced to the only dominant modes. This typically happens when multiple discontinuities are cascaded together at short distances. Higher-order mode interaction takes place between adjacent discontinuities in such a way that active power may be carried by higher-order modes. In such cases, a more general description of the discontinuity is needed.

To obtain a terminal description of the discontinuity in the general case, it is worth recalling that each waveguide mode can be represented by an equivalent transmission line, the voltage and current amplitudes being proportional to the modal electric and magnetic field amplitudes, respectively

$$\mathbf{E}_t^{(i)}(x, y, z) = \sum_m V_m^{(i)}(z) \mathbf{e}_m^{(i)}(x, y) \quad (1)$$

$$\mathbf{H}_t^{(i)}(x, y, z) = \sum_m I_m^{(i)}(z) \mathbf{h}_m^{(i)}(x, y) \quad (2)$$

where z is the longitudinal axis of the waveguide, $\mathbf{E}_t^{(i)}$ and $\mathbf{H}_t^{(i)}$ are the transverse electric and magnetic fields, $V_m^{(i)}$ and $I_m^{(i)}$ are the voltage and current of the transmission line equivalent to the m th mode of the i th waveguide, and $\mathbf{e}_m^{(i)}$ and $\mathbf{h}_m^{(i)}$ are the transverse electric and magnetic modal vectors.

Although in principle an infinite series of modes is involved in the electromagnetic field representation, in practice only a finite number of modes need to be taken into account to achieve a prescribed accuracy. As a consequence, the electromagnetic field distribution over each terminal plane is expressed in terms of a finite number of voltage and current amplitudes. Let N_i be the number of modes taken into account in the field description at the i th terminal plane ($i = 1, 2$); the terminal description of the discontinuity will involve $N_1 + N_2$ voltages and the same number of currents. Because of the linearity of Maxwell's equations, these quantities are related by a linear set of $N_1 + N_2$ equations. One can easily realize that Maxwell's equations lead to $N_1 + N_2$ equations by the following reasoning. By virtue of the unicity theorem for electromagnetic fields, the entire electromagnetic field distribution in the structure is determined by the the knowledge of the tangential electric (or magnetic) field at the two terminal planes, thus by the knowledge of the whole set of $N_1 + N_2$ voltages (or currents) over such planes. In other words, from the knowledge of $N_1 + N_2$ voltages (currents) one can compute the $N_1 + N_2$ currents (voltages). This implies that the linear system consists of $N_1 + N_2$ equations relating the $N_1 + N_2$ voltages to the $N_1 + N_2$ currents.

The modal approach lends itself to the so-called microwave network formalism. The discontinuity, rather than the electric and magnetic field distribution, is described in terms of voltages and currents, that is, as a multiport circuit [Fig. 1(b)]. In the equivalent circuit of Fig. 1(b) each port corresponds to a mode excited at one of the terminal planes of the discontinuity. The system can be put in many different forms. One of the most convenient approaches consists of expressing currents in terms of voltages. In matrix form this corresponds to writing

$$[I] = [Y] \cdot [V] \quad (3)$$

4 WAVEGUIDE DISCONTINUITIES

where $[I]$ is the vector of the currents, $[V]$ that of the voltages and $[Y]$ the admittance matrix. For the case of the two-terminal-plane network of Fig. 1(a) the vector of the currents is

$$[I] = \begin{bmatrix} [I^{(1)}] \\ [I^{(2)}] \end{bmatrix} \quad (4)$$

The subvector of the currents at the i th terminal plane ($i = 1, 2$) is

$$[I^{(i)}] = [I_1^{(i)}, I_2^{(i)}, \dots, I_{N_i}^{(i)}]^T \quad (5)$$

with N_i being the number of modes (or electrical ports) considered at the i th plane. The voltage vector is similar to the current vector, and the admittance matrix is composed by four submatrices as follows:

$$[Y] = \begin{bmatrix} [Y^{(11)}] & [Y^{(12)}] \\ [Y^{(21)}] & [Y^{(22)}] \end{bmatrix} \quad (6)$$

Observe that while the electromagnetic structure has two outputs (or two apertures), the equivalent circuit has $N_1 + N_2$ electric ports.

In most practical cases the terminal planes are chosen far enough from the discontinuity in such a way that higher-order modes have vanished. This is possible whenever the discontinuity is isolated, that there are no other discontinuities close to it. The electromagnetic field at the terminal planes is that of the dominant modes of the respective waveguides, while higher-order modes have died out. In the multiport equivalent circuit description of Fig. 1(b), this situation corresponds to terminating the higher-order mode ports with their characteristic impedances. The multiport description reduces to the two-port description of Fig. 1(c), where the accessible ports represent the dominant modes of both waveguides.

To compute the 2×2 admittance matrix of Fig. 1(c) from the $(N_1 + N_2) \times (N_1 + N_2)$ admittance matrix of Fig. 1(b), the matching conditions at the higher-order mode ports are added to Eq. (3):

$$I_m^{(i)} = -y_{c,m}^{(i)} V_m^{(i)} \quad (7)$$

In Eq. (7) $y_{c,m}^{(i)}$ is the characteristic admittance of the equivalent transmission line, which has been assumed as the wave impedance of the waveguide mode

$$y_{c,m}^{(i)} = \begin{cases} \beta_m^{(i)} / \omega \mu, & \text{TE modes} \\ \omega \epsilon / \beta_m^{(i)}, & \text{TM modes} \end{cases} \quad (8)$$

with

$$\beta_m^{(i)} = \sqrt{\left(\frac{\omega}{c}\right)^2 - (k_{c,m}^{(i)})^2} \quad (9)$$

where c is the velocity of light, $\beta_M^{(i)}$ the phase constant, and $k_{c,m}^{(i)}$ the eigenvalue of the m th mode.

After rearranging and partitioning the admittance matrix, Eq. (6), according to fundamental (subscript f) and higher-order modes (subscript h)

$$[Y] = \begin{bmatrix} [Y_{ff}] & [Y_{fh}] \\ [Y_{hf}] & [Y_{hh}] \end{bmatrix} \quad (10)$$

the two-port admittance matrix description $[Y']$ of the discontinuity is easily obtained from Eqs. (7) and (3)

$$[Y'] = [Y_{ff}] - [Y_{fh}] \cdot ([Y_{hh}] + [Y_c])^{-1} \cdot [Y_{hf}] \quad (11)$$

where $[Y_c]$ is the diagonal matrix of the characteristic admittances of the higher-order modes

$$[Y_c] = \text{diag} [y_{c,2}^{(1)}, \dots, y_{c,N_1}^{(1)}, y_{c,2}^{(2)}, \dots, y_{c,N_2}^{(2)}] \quad (12)$$

Alternative descriptions of the discontinuity can be obtained either by rearranging the discontinuity equations or by using different electrical quantities rather than voltages and currents. In the former case, an impedance matrix description is obtained by expressing the voltages in terms of the currents

$$[V] = [Z] \cdot [I] \quad (13)$$

By expressing the waveguide fields in terms of incident $[a]$ and reflected $[b]$ wave vectors one can obtain a scattering matrix description of the discontinuity

$$[b] = [S] \cdot [a] \quad (14)$$

The incident and reflected waves are related to voltage and current amplitudes as

$$a_m^{(i)} = \frac{y_{c,m}^{(i)} V_m^{(i)} + I_m^{(i)}}{2\sqrt{y_{c,m}^{(i)}}} \quad (15)$$

$$b_m^{(i)} = \frac{y_{c,m}^{(i)} V_m^{(i)} - I_m^{(i)}}{2\sqrt{y_{c,m}^{(i)}}} \quad (16)$$

with $i = 1, 2$, and $m = 1, \dots, N_i$. The interrelations among the above matrix description are

$$\begin{aligned} [\tilde{Y}] &= [\tilde{Z}]^{-1} = ([U] + [S])^{-1} \cdot ([U] - [S]) \\ [\tilde{Z}] &= [\tilde{Y}]^{-1} = ([U] + [S]) \cdot ([U] - [S])^{-1} \\ [S] &= ([\tilde{Z}] - [U]) \cdot ([\tilde{Z}] + [U])^{-1} = ([U] + [\tilde{Y}])^{-1} \cdot ([U] - [\tilde{Y}]) \end{aligned} \quad (17)$$

where $z_{c,m}^{(i)} = 1/y_{c,m}^{(i)}$ is the characteristic impedance of the equivalent transmission line.

The use of a lumped or distributed element equivalent-circuit model to describe the discontinuity can be advantageous for many practical applications. The circuit model can be easily handled in more conventional

6 WAVEGUIDE DISCONTINUITIES

engineering terms, and when properly derived, reflects the physical behavior of the discontinuity. Moreover, it has the advantage of easily providing by mere inspection a description of the behavior of the discontinuity and the way the latter can be used for practical applications (e.g., filters).

From this discussion it is apparent that a certain degree of arbitrariness is involved in the choice of the reference planes. As a consequence, different equivalent circuits can be assumed, depending on the location of the terminal planes. A proper choice of the reference plane locations can be used in some cases in order to reduce the complexity of the equivalent-circuit. This ambiguity is inherent to the distributed nature of waveguide circuits, as opposed to lumped low-frequency circuits, where no ambiguity exists.

An additional ambiguity in the definition of the equivalent circuit models resides in the arbitrariness in the definition of the equivalence between waveguide mode and transmission line. In particular, the characteristic impedance $z_{c,m}^{(i)}$ of the m th transmission line can be changed by a factor of n^2 by transforming the voltages $V_m^{(i)}$ and currents $I_m^{(i)}$ into a new set $\hat{V}_m^{(i)}$ and $\hat{I}_m^{(i)}$

$$\hat{Y}_{mn}^{(ij)} = \frac{Y_{mn}^{(ij)}}{\sqrt{y_{c,m}^{(i)} y_{c,n}^{(j)}}} \quad (18)$$

$$\hat{Z}_{mn}^{(ij)} = \frac{Z_{mn}^{(ij)}}{\sqrt{z_{c,m}^{(i)} z_{c,n}^{(j)}}} \quad (19)$$

so that

$$\hat{V}_m^{(i)} = n V_m^{(i)} \quad (20)$$

The new definition is equivalent to the introduction of ideal transformers at the circuit terminals. By an appropriate selection of both the reference planes and the voltage–current definitions, different equivalent circuits with reduced complexity can be derived.

In the presence of multiple or cascaded discontinuities special caution should be employed in the use of the equivalent-circuit models. If adjacent discontinuities are cascaded at a short distance, in fact, the reference planes cannot be chosen far enough from the discontinuities to make higher-order modes vanish. In this case, discontinuities interact through higher-order modes. The models for isolated discontinuities may lead to significant errors. Multiport equivalent networks including higher-order mode interactions must be adopted instead. This is illustrated with a specific example in the section Isolated and Interacting Discontinuities.

General Properties of Waveguide Discontinuities

This section presents a brief description of the general properties of waveguide discontinuities.

Losslessness. Losses in microwave circuits are due to imperfect dielectric materials (dielectric loss), finite conductivity of the conductors (conductor loss), and, for open structures, radiation (radiation loss). The impedance or admittance matrices of lossy discontinuities possess real and imaginary parts that are associated with the real and the reactive power, respectively.

In many practical cases losses may be neglected with good approximation so that the discontinuity behaves as a reactive circuit. The admittance and the impedance matrices are purely imaginary and the scattering matrix is unitary. The latter property is obtained by expressing the balance between incident and

reflected power in terms of wave vectors, Eqs. (15) and (16), as

$$\Gamma_m^{(i)} = \frac{1}{n} I_m^{(i)} \quad (21)$$

Using Eq. (14) one obtains the unitarity condition for the scattering matrix of a lossless discontinuity

$$\hat{z}_{c,m}^{(i)} = n^2 z_{c,m}^{(i)*} \quad (22)$$

In Eqs. (23) and (24) the asterisk stands for complex conjugate.

Reciprocity. As long as Lorentz's reciprocity theorem holds for the region occupied by the discontinuity, the latter behaves as a reciprocal network. This implies that the admittance, impedance, and scattering matrices are symmetrical. As a consequence, a reciprocal N -port discontinuity is characterized by $N(N + 1)/2$ complex parameters. Such parameters reduce to real parameters for lossless structures. Discontinuities containing anisotropic materials such as ferrite are examples of nonreciprocal circuits that are characterized by nonsymmetrical matrix descriptions.

Symmetry. The presence of geometrical symmetries of a discontinuity can be exploited to reduce the complexity of its analysis, as well as the number of unknown parameters of its equivalent network representation. For example, in the case of a two-port discontinuity, the existence of a central symmetry plane between the two outputs implies a corresponding symmetry of the matrix representations, provided that the terminal planes are chosen symmetrically (e.g. $Y_{11} = Y_{22}$). In such a case, the discontinuity, if reciprocal, is characterized by only two rather than three parameters, as in the general case. For a more detailed discussion on the exploitation of symmetry planes in three- or four-port structures, the reader is referred to Ref. 7, Sec. 3.2.

Categorization of Waveguide Discontinuities

There is no unique way to classify waveguide discontinuities, since a number of different criteria can be adopted. Here we attempt at a categorization of discontinuities with reference to some geometrical characteristics that are somewhat related to the corresponding electromagnetic problem. Examples of common discontinuities are shown in Tables 1 to 5. The examples discussed here are not exhaustive but represent just a small fraction of what can be found in practical applications. The reader is also provided with some representative references taken from the immense amount of technical publications on this topic.

Uniaxial Junctions. In a uniaxial junction, two waveguides with different cross sections and coincident longitudinal axes are connected together. In the case of rectangular waveguides, examples of such discontinuities are the E -plane (or capacitive) step (12,14,15), the H -plane (or inductive) step (16), and E -plane and H -plane offsets. These discontinuities are illustrated in Table 1. As long as both waveguides are in the single-mode regime, the corresponding equivalent networks have two ports. Other examples of uniaxial discontinuities are the junction between two circular waveguides (12), the junction between a coaxial cable and a circular waveguide (17), and the junction between a rectangular waveguide and a circular waveguide (18,19).

Bifurcations and N -Furcations. One waveguide is joined to two or more waveguides with parallel longitudinal axes. A theoretical model of N -furcations has been presented in Ref. 20. In rectangular waveguide the bifurcation can occur in either the E or the H plane, as shown in Table 2. The equivalent circuit may contain more than three ports, because the larger waveguide may support the propagation of higher-order modes.

Obstacles. Metallic or dielectric obstacles can be inserted in a waveguide to achieve specific electrical behaviors. Metallic obstacles may have infinitesimal or finite length along the waveguide axis. In the former

8 WAVEGUIDE DISCONTINUITIES

Table 1. Uniaxial Junctions in Rectangular Waveguides

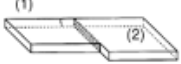

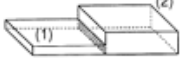
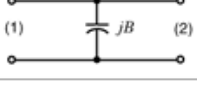

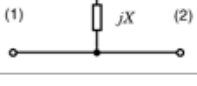
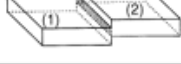
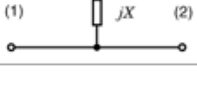
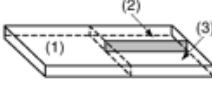
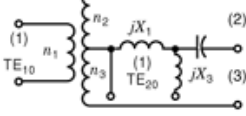
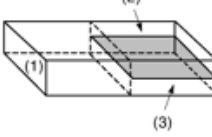
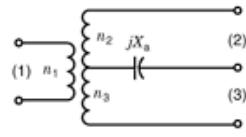
Name	Structure	Equivalent circuit	References
<i>H</i> -plane step			7, pp. 296–302
<i>E</i> -plane step			7, pp. 307–310
<i>H</i> -plane offset			
<i>E</i> -plane offset			

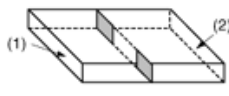
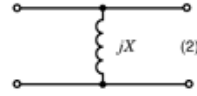

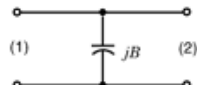
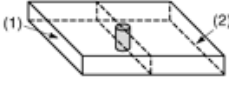
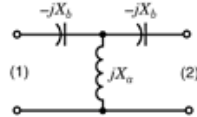
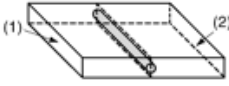
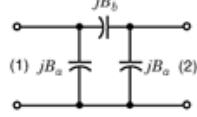
Table 2. Bifurcations in Rectangular Waveguides

Name	Structure	Equivalent circuit	References
<i>H</i> -plane bifurcation			7, pp. 382–386 TE ₁₀ mode in all waveguides, in addition, TE ₂₀ mode in the larger waveguide
<i>E</i> -plane bifurcation			7, pp. 353 – 355

case the equivalent circuit can be reduced to a shunt admittance. Typical examples are metal irises and metal posts. They have been widely employed as filter and matching network elements. In the case of rectangular waveguides, depending on the orientation with respect to the electric field of the dominant mode, such obstacles exhibit inductive or capacitive behavior, as shown in Table 3. Observe that irises are supposed to be infinitesimally thin. A full-wave model of the inductive iris in rectangular waveguide can be found in Refs. 12 and 21. More complicated geometries involving circular irises (22,23) and slanting and multiple rectangular irises (24,25) in rectangular waveguides, as well as irises in coaxial cables (26) and circular waveguides (27,28) have been investigated. Electromagnetic models of posts in rectangular waveguide can be found in, Refs. 29,30,31.

Multiaxial Junctions. Two or more waveguides with different longitudinal axes are connected together (see Table 4). In the case of uniaxial junctions, the associated boundary-value problem is a two-dimensional (2-D) one. In the case of multiaxial junctions, in contrast, the analysis involves the solution of a 3-D boundary-value problem. The simplest case of a biaxial junction is the right-angle junction between two rectangular waveguides. Depending on the plane of such junction, we have an *E*-plane or *H*-plane corner. This type of

Table 3. Obstacles

Name	Structure	Equivalent circuit	References
Inductive iris			7, pp. 221-229
Capacitive iris			7, pp. 218-221
Inductive post			7, pp. 257-266
Capacitive post			7, pp. 268-271

discontinuity effects a 90° change of direction in the waveguide axis. To minimize reflections alternative geometries can be adopted, such as the mitered bends (32,33) and the circular bends (34,35).

More complicated multiaxial junctions in rectangular waveguide technology are the T junctions in the *E*-plane (36,37,38) or in the *H*-plane (39,40,41). The matching of such junctions has been analyzed in detail in Ref. 42. The so-called magic (hybrid) Tee is a well-known rectangular waveguide component where ports are decoupled in pairs (43). The aperture in the common wall of two rectangular waveguides (44, 45) can also be seen as an example of four-port multiaxial junction. An example of a T junction between rectangular and circular waveguide has been investigated in Ref. 46.

Open Discontinuities. In the examples presented so far, the discontinuities were completely bounded by metallic walls. An important category of waveguide discontinuities, however, is represented by open discontinuities, where the electromagnetic field can be radiated in the outer space. The equivalent circuits of such discontinuities contain resistors that represent the radiation loss. Some examples are illustrated in Table 5.

One example is the open-ended waveguide. When the electromagnetic field impinges on such a termination, part of the associated power is reflected and part is radiated in the free space, so that the termination can be considered as an antenna. Such terminations, in fact, are widely used as secondary antennas (feeding antennas) in reflector-type antennas or as elements of an array antenna. The study of the radiation mechanism is rather complicated, and electromagnetic full-wave models are mandatory. The reader is referred to Refs. (47,48,49) for rectangular waveguides and to Refs. 50 and 51 for coaxial and circular waveguide.

Other radiating discontinuities are obtained by producing apertures in the waveguide walls. The aperture interrupts locally the conduction current flowing on the walls, producing both a distortion in the lines of flux as well as a displacement current in the aperture. The latter is necessary to maintain the continuity of the total current and constitutes the source of the radiated electromagnetic field. The most common example is the radiating slot in rectangular waveguide. The longitudinal slot in the broad wall has been analyzed in Refs. 52,53,54, the slanting slot in Refs. 55, and the transverse slot has been investigated in Refs. 56 and 57.

10 WAVEGUIDE DISCONTINUITIES

Table 4. Multiaxial Junctions

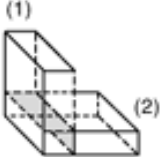
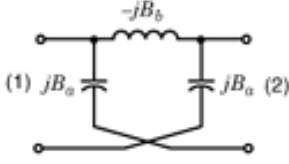
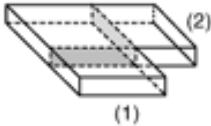
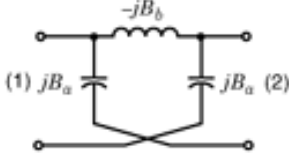
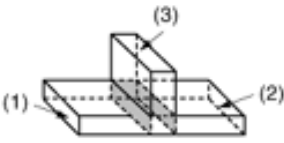
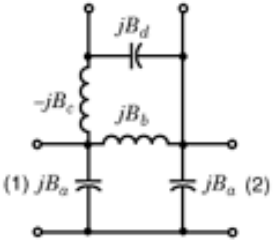
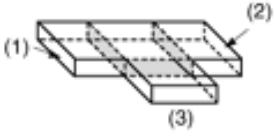
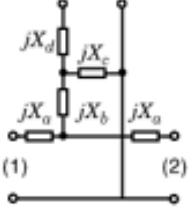
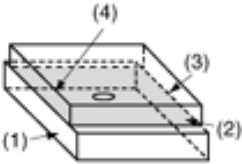
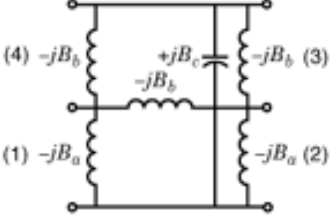
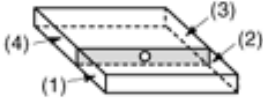
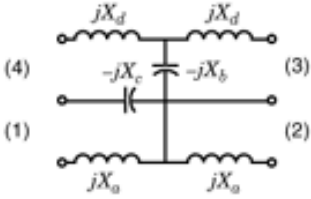
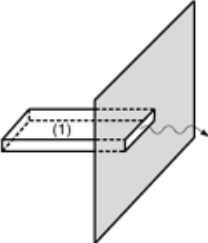
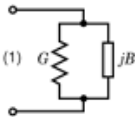
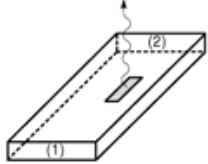
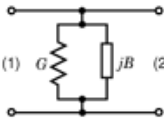
Name	Structure	Equivalent circuit	References
E-plane corner			7, pp. 312–318
H-plane corner			7, pp. 318–322
E-plane Tee			7, pp. 337–338
H-plane Tee			7, pp. 355–356
Coupling hole E plane			7, pp. 375–376
Coupling hole H plane			7, pp. 379–380

Table 5. Radiating Discontinuities

Name	Structure	Equivalent circuit	References
Open waveguide (with flange)			7, pp 193–194
Longitudinal slot			53

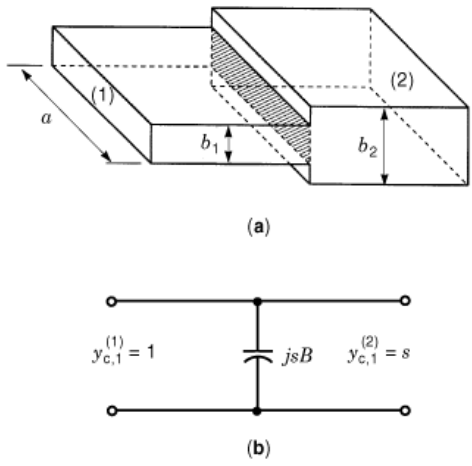


Fig. 2. Capacitive step in rectangular waveguide: (a) structure; (b) equivalent circuit. Geometrical dimensions: $a = 19.05$ mm, $b_2 = 9.52$ mm, $b_1 = sb_2$.

Isolated and Interacting Discontinuities

Earlier it was pointed out that the reduced equivalent circuit valid for an isolated discontinuity may not be adopted, in general, for adjacent discontinuities, because of the higher-order mode interaction occurring between them. To illustrate this phenomenon, consider as an example the symmetrical capacitive step in a rectangular waveguide depicted in Fig. 2(a) The larger waveguide is the WR75 waveguide operating in the 10 GHz to 15 GHz frequency range. The equivalent circuit of the step, assumed to be isolated, is shown in Fig. 2(b).

12 WAVEGUIDE DISCONTINUITIES

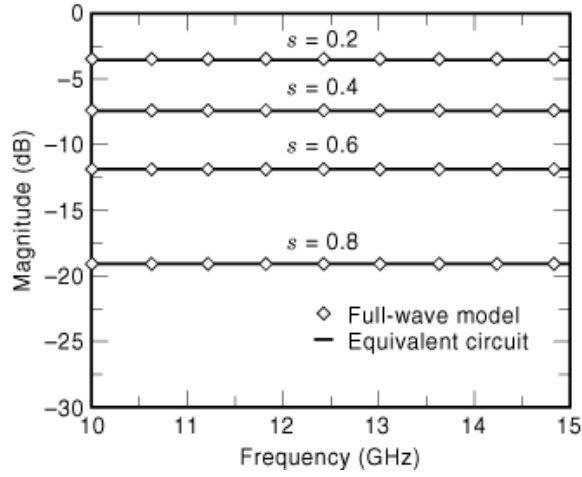


Fig. 3. S_{11} of a capacitive step in a rectangular waveguide for various step ratios $s = b_1/b_2$. Comparison between the equivalent circuit and the full-wave mode-matching analysis.

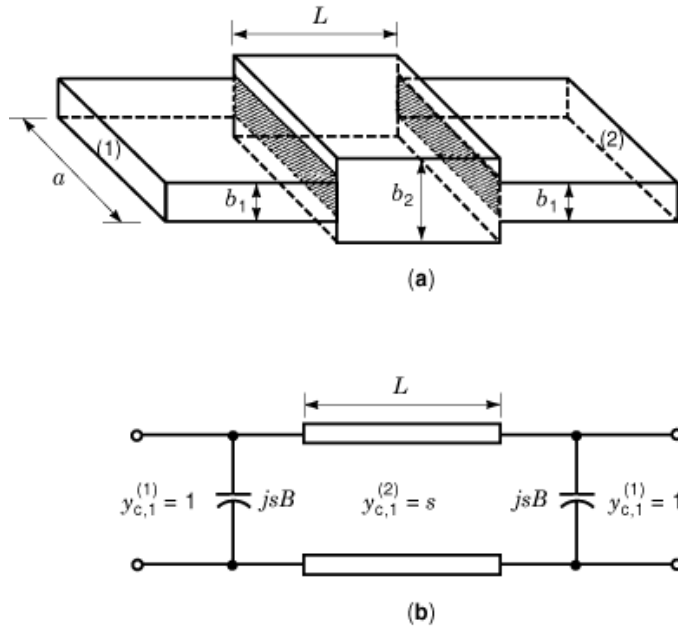


Fig. 4. Capacitive double step in rectangular waveguide (a) structure; (b) equivalent circuit. Geometrical dimensions: $a = 19.05$ mm, $b_2 = 9.52$ mm, $b_1 = 1.90$ mm, $s = 0.20$.

The shunt capacitance represents the reactive energy stored in the proximity of the step, due to attenuated higher-order modes excited at the junction between the two waveguides. The step susceptance is sB , s being the step ratio

$$\frac{1}{2}[a]^T \cdot [a]^* = \frac{1}{2}[b]^T \cdot [b]^* \quad (23)$$

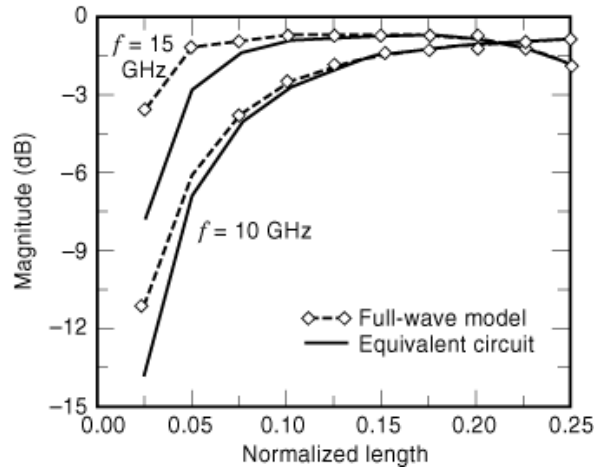


Fig. 5. S_{11} of the double step versus the normalized length L/λ_{c0} of the central waveguide. Comparison between the equivalent circuit and the full-wave mode-matching analysis.

and B is easily computed by the approximate formula given in Ref. 7, p. 307. The scattering parameter S_{11} of the discontinuity can be evaluated by elementary network analysis

$$[S]^T \cdot [S]^* = [U] \quad (24)$$

This parameter is shown in Fig. 3 as a function of frequency for different step ratios. For comparison, the scattering parameter computed by the rigorous mode-matching technique is also shown. The approximate formula is shown to be very accurate compared with the computationally more expensive mode-matching method.

Let us now consider two capacitive steps cascaded through a uniform waveguide of length L [Fig. 4(a)]. The step ratio is $s = b_1/b_2 = 0.2$. The cascaded steps have been analyzed both by the equivalent circuit of Fig. 4(b) and by the mode-matching method. In the former case the higher-order mode interaction between the two steps is totally neglected, while, in the latter case, higher order mode interaction has been fully taken into account. Figure 5 shows the computed scattering parameter $S_{11} = S_{22}$ as a function of the normalized length L/λ_{c0} at the lower (10 GHz) and upper (15 GHz) ends of the frequency range of the WR75 waveguide. $\lambda_{c0} = 2a = 39$ mm is the cutoff wavelength of the waveguide. It is observed that the equivalent circuit of Fig. 4(b), based on the hypotheses of isolated discontinuities, is accurate as long as the normalized distance exceeds $\lambda_{c0}/8$. For lower distances, the error increases and becomes unacceptable below $\lambda_{c0}/20$. It can be noted that the error increases with frequency, as a result of the stronger excitation of higher-order modes.

BIBLIOGRAPHY

1. C. G. Montgomery, R. H. Dicke, E. M. Purcell, *Principles of Microwave Circuits*, New York: McGraw-Hill, 1948.
2. L. Lewin, *Advanced Theory of Waveguides*, London: Iliffe, 1951.
3. R. Mittra S. W. Lee, *Analytical Techniques in the Theory of Guided Waves*, New York: Macmillan 1971.
4. R. E. Collin, *Field Theory of Guided Waves*, Piscataway, NJ: IEEE Press, 1990.
5. D. Pozar, *Microwave Engineering*, Reading, MA: Addison-Wesley, 1990.
6. R. E. Collin, *Foundations for Microwave Engineering*, New York: McGraw-Hill, 1992.
7. N. Marcuvitz, *Waveguide Handbook*, New York: McGraw-Hill, 1951.

14 WAVEGUIDE DISCONTINUITIES

8. T. Itoh, *Numerical Techniques for Microwave and Millimeter Wave Passive Components*, New York: Wiley, 1988.
9. M. Sorrentino, *Numerical Methods for Passive Microwave and Millimeter Wave Structures*, New York: IEEE Press, 1989.
10. M. Sadiku, *Numerical Techniques in Electromagnetics*, Boca Raton, FL: CRC Press, 1992.
11. A. Wexler, Solution of waveguide discontinuities by modal analysis, *IEEE Trans. Microw. Theory Tech.*, **15**: 508–517, 1967.
12. P. H. Mastermann P. J. B. Clarricoats, Computer field-matching solution of waveguide transverse discontinuities, *IEE Proc.*, **118**: 51–63, 1971.
13. R. Sorrentino, *et al.* An investigation of the numerical properties of the mode-matching technique, *Int. J. Numerical Modelling*, **4**: 19–43, 1991.
14. T. Rozzi M. Mongiardo, E-plane steps in rectangular waveguide, *IEEE Trans. Microw. Theory Tech.*, **39**: 1279–1288, 1991.
15. M. Guglielmi G. Gheri, Rigorous multimode network representation of capacitive step, *IEEE Trans. Microw. Theory Tech.*, **42**: 622–628, 1994.
16. M. Guglielmi, *et al.* Rigorous multimode network numerical representation of inductive step, *IEEE Trans. Microw. Theory Tech.*, **42**: 317–326, 1994.
17. J. D. Mahony, A low-frequency investigation into the discontinuity capacitance of a coaxial line terminated in a lossless, dielectric loaded circular guide, *IEEE Trans. Microw. Theory Tech.*, **35**: 344–346, 1987.
18. J. L. Fontecha C. Caligal, Transition rectangular to circular waveguide by means of rectangular guide, in *Int. Conf. Computation Electromagn.*, Nov. 1991, pp. 378–391.
19. P. Guillot, *et al.* Improvement in calculation of some surface integrals: Application to junction characterization in cavity filter design, *IEEE Trans. Microw. Theory Tech.*, **41**: 2156–2160, 1993.
20. F. Dai, Scattering and transmission matrix representations of multiguide junctions, *IEEE Trans. Microw. Theory Tech.*, **40**: 1538–1544, 1992.
21. M. Guglielmi C. Newport, Rigorous, multimode equivalent network representation of inductive discontinuities, *IEEE Trans. Microw. Theory Tech.*, **38**: 1651–1659, 1990.
22. C. Sabatier, Scattering at an offset circular hole in a rectangular waveguide, *IEEE Trans. Microw. Theory Tech.*, **40**: 587–592, 1992.
23. U. Papziner F. Arndt, Field theoretical computer-aided-design of rectangular and circular iris coupled rectangular or circular waveguide cavity filters, *IEEE Trans. Microw. Theory Tech.*, **41**: 462–471, 1993.
24. R. Yang A. S. Omar, Analysis of thin inclined rectangular aperture with arbitrary location in rectangular waveguide, *IEEE Trans. Microw. Theory Tech.*, **41**: 1461–1463, 1993.
25. R. Yang A. S. Omar, Investigation of multiple rectangular aperture irises in rectangular waveguide using TE modes, *IEEE Trans. Microw. Theory Tech.*, **41**: 1369–1374, 1993.
26. G. L. James, Admittance of irises in coaxial and circular waveguide for TE₁₁ mode excitation, *IEEE Trans. Microw. Theory Tech.*, **35**: 430–434, 1987.
27. R. W. Scharstein A. T. Adams, Thick circular iris in a TE₁₁ mode circular waveguide, *IEEE Trans. Microw. Theory Tech.*, **36**: 1529–1531, 1988.
28. Z. Shen R. H. MacPhie, Scattering by a thick off-centered circular iris in circular waveguide, *IEEE Trans. Microw. Theory Tech.*, **43**: 2639–2642, 1995.
29. J.-W. Tao H. Baudrand, Multimodal variational analysis of uniaxial waveguide discontinuities, *IEEE Trans. Microw. Theory Tech.*, **39**: 506–516, 1991.
30. T. Rozzi, *et al.* Accurate full-band equivalent circuit of inductive posts in rectangular waveguide, *IEEE Trans. Microw. Theory Tech.*, **40**: 1000–1009, 1992.
31. H.-W. Yao *et al.*, Full wave modeling of conducting posts in rectangular waveguide and its application to slot coupled combline filters, *IEEE Trans. Microw. Theory Tech.*, **43**: 2824–2830, 1995.
32. J. M. Reiter F. Arndt, A full-wave boundary contour mode-matching method BCMM for the rigorous CAD of single and cascaded optimized H-plane and E-plane bends, *IEEE Int. Microw. Symp.*, San Diego, CA, 1994, pp. 1021–1024.
33. F. Alessandri, M. Mongiardo, R. Sorrentino, Rigorous mode matching analysis of mitered E-plane bends in rectangular waveguide, *IEEE Microwave Guided Wave Lett.*, **4**: 408–410, 1994.
34. M. Mongiardo, A. Morini, T. Rozzi, Analysis and design of full-band matched waveguide bends, *IEEE Trans. Microw. Theory Tech.*, **43**: 2965–2971, 1995.

35. B. Gimeno M. Guglielmi, Multimode equivalent network representation for H- and E-plane uniform bends in rectangular waveguide, *IEEE Trans. Microw. Theory Tech.*, **44**: 1679–1687, 1996.
36. E. D. Sharp, An exact calculation for a T-junction of rectangular waveguides having arbitrary cross sections, *IEEE Trans. Microw. Theory Tech.*, **15**: pp. 109–116, 1967.
37. T. Obata J. Chita, Improved theory for E-plane symmetrical tee junctions, *IEEE Trans. Microw. Theory Tech.*, **37**, 624–627, 1989.
38. P. Lampariello A. A. Oliner, New equivalent network with simple closed-form expressions for open and slit-coupled E-plane tee junctions, *IEEE Trans. Microw. Theory Tech.*, **41**: 839–847, 1993.
39. B. N. Das N. V. S. N. Sarma, Analysis of E-H plane tee junction using a variational formulation, *IEEE Trans. Microw. Theory Tech.*, **39**, 1770–1773, 1991.
40. X.-P. Liang, K. A. Zaki, A. E. Atia, A rigorous three plane mode-matching technique for characterizing waveguide T junctions, and its application in multiplexer design, *IEEE Trans. Microw. Theory Tech.*, **39**: 2138–2147, 1991.
41. T. Sieverding F. Arndt, Field theoretical CAD of open or aperture matched T-junction coupled rectangular waveguide structures, *IEEE Trans. Microw. Theory Tech.*, **40**: 353–362, 1992.
42. J. Hirokawa et. al, An analysis of a waveguide T junction with an inductive post, *IEEE Trans. Microw. Theory Tech.*, **39**: 563–566, 1991.
43. J. M. Rebollar, J. Esteban, J. Page, Fullwave analysis of three and four-port rectangular waveguide junctions, *IEEE Trans. Microw. Theory Tech.*, **42**: 256–263, 1994.
44. A. Datta, et al. S. matrix of a broad wall coupler between dissimilar rectangular waveguides, *IEEE Trans. Microw. Theory Tech.*, **43**: 56–62, 1995.
45. A. M. Rajeev A. Chakrabarty, Analysis of wide compound slot-coupled parallel waveguide coupler and radiator, *IEEE Trans. Microw. Theory Tech.*, **43**: 802–809, 1995.
46. B. N. Das., P. V. D. S. Rao, A. Chakraborty, Narrow wall axial-slot-coupled T junctions between rectangular and circular waveguides, *IEEE Trans. Microw. Theory Tech.*, **37**, 1590–1596, 1989.
47. H. Baudrand, J.-W. Tao, J. Atechian, Study on radiating properties of open-ended rectangular waveguides, *IEEE Trans. Antennas Propag.*, **36**: 1071–1077, 1988.
48. B. N. Das, A. Chakraborty, S. Gupta, Analysis of waveguides-fed thick radiating rectangular windows in a ground plane, *IEE Proc. H*, **138**: 142–146, 1991.
49. M. Mongiardo T. Rozzi, “Singular integral equation analysis of flange-mounted rectangular waveguide radiators,” *IEEE Trans. Antennas Propag.*, **41**: 556–565, 1993.
50. T. B. Bird, Cross-coupling between open-ended coaxial radiators, *IEE Proc. Microw. Antennas Propag.*, **143**: 265–271, 1996.
51. T. S. Bird, Improved solution for mode coupling in different-sized circular apertures and its application, *IEE Proc. Microw. Antennas Propag.*, **143**: 457–464, 1996.
52. G. J. Stern R. S. Elliot, Resonant length of longitudinal slots and validity of circuit representation: Theory and experiment, *IEEE Trans. Antennas Propag.*, **33**: 1264–1271, 1985.
53. L. G. Josefsson, Analysis of longitudinal slots in rectangular waveguides, *IEEE Trans. Antennas Propag.*, **35**: 1351–1357, 1987.
54. R. Kastner, On the convergence of matrix elements in planar and waveguide problems, *IEE Proc. H*, **138**: 532–536, 1991.
55. S. R. Rengarajan, Compound radiating slots in a broad wall of a rectangular waveguide, *IEEE Trans. Antennas Propag.*, **37**: 1116–1123, 1989.
56. L. G. Josefsson, A waveguide transverse slot for array application, *IEEE Trans. Antennas Propag.*, **41**: 845–850, 1993.
57. J. Joubert, A transverse slot in the broad wall of inhomogeneously loaded rectangular waveguide for array application, *IEEE Microwave Guided Wave Lett.*, **5**: 37–39, 1995.

ROBERTO SORRENTINO
FEDERICO ALIMENTI
University of Perugia